Confined diffusion of erbium excitations in SnO_2 nanoparticles embedded in silica: A time-resolved infrared luminescence study

S. Brovelli,[1,2] N. Chiodini,[1] F. Meinardi,[1] A. Monguzzi,[1] A. Lauria,[1] R. Lorenzi,[1] B. Vodopivec,[1] M. C. Mozzati,[3] and A. Paleari[1]

[1]*CNISM–Department of Materials Science, University of Milano-Bicocca, Via R. Cozzi 53, I-20125 Milano, Italy*

[2]*London Centre for Nanotechnology, and Department of Physics and Astronomy, University College London, Gower Street, London WC1E 6BT, United Kingdom*

[3]*CNISM–Department of Physics "Alessandro Volta," University of Pavia, via Bassi 6, I-27100 Pavia, Italy*

(Received 19 January 2009; published 24 April 2009)

We have identified, in erbium-doped silica with SnO_2 nanocrystals, excitation-diffusion processes restricted to the single nanocrystal. Time-resolved measurements of erbium infrared luminescence excited by energy transfer via nanocrystal excitation, together with the identification and quantification of the nanophase-related Er^{3+} variety by its electron paramagnetic resonance, have allowed us to analyze the dependence of the excitation decay rate on the number of ions per nanoparticle and to reveal the effects of the discrete spatial domain composed by nanocrystals. Finally, a nonlinear relation is derived to describe the effects of Förster energy transfer in disconnected nanosystems.

DOI: 10.1103/PhysRevB.79.153108 PACS number(s): 78.67.Bf, 62.23.Pq, 76.30.Kg, 78.47.Cd

Förster resonant energy transfer (FRET) is a physical mechanism consisting of the exchange of energy from an excited system to another without photon exchange.[1] In optical materials this mechanism plays an important role in determining the excitation diffusion within a variety of similar atomic or molecular sites and the excitation transfer from donor to acceptor sites of different species. Interesting properties and applications in several fields are based on FRET from advanced experimental methods for cell and molecule detection[2] to the design of materials for optical amplification.[3] An important extension of the FRET mechanism concerns nanostructured materials where energy transfer from nanoparticle excitons leads to strongly sensitized light emission from optically active ions, thus enabling optical gain[4,5] and electroluminescence.[6,7] For this reason, energy transfer in nanostructured systems, especially erbium-doped silica-based compounds, has been investigated by several groups, both in material produced by chemical vapor deposition[3,8–12] and in materials produced via sol gel.[13–15] Nevertheless, FRET mechanisms are also responsible for energy migration from ion to ion and may lead to large excitation diffusion within an ensemble of optically active sites. This process is potentially detrimental for applications as it may drive the excitation toward nonradiative decay in quenching sites with the resulting reduction of the quantum efficiency of light-emitting systems. A breakthrough in this field would be the realization of nanostructured systems that were able to both transfer excitation from the nanophase to optically active species and confine the excitation diffusion within the single nanosystem. However, not only is the feasibility of such systems still to be demonstrated but it is not yet clear which features the excitation diffusion should exploit if confined in a region of a few nm, comparable with the Förster radius.

In this work we demonstrate the feasibility of a nanostructured system with nanoparticle-confined excitation diffusion and identify the main features of the excitation-diffusion process when constrained in an ensemble of disconnected nanosystems. To do this, we have investigated Er-doped SiO_2 with embedded SnO_2 nanoparticles, where erbium ions have a role both as functional species for delivering sensitized fluorescence,[13,16] and as agents in defining nanomorphology.[17–20] Here we show that the excitation diffusion within the erbium variety excited via FRET from nanoparticle excitons is confined in the single nanocrystal without appreciable energy transfer to erbium ions in the glass. The results indicate that the excitation-diffusion rate depends on the number of ions per nanoparticle with a sublinear dependence that can be ascribed to the discreteness of the spatial domain.

Samples of Er-doped silica with SnO_2 nanocrystals were prepared by a sol-gel technique with 8 mol % of SnO_2 and erbium content ranging from 500 ppm to 1 mol % by cogelling tetraethoxysilane, dibutyl tin diacetate, and erbiumnitrate. After gelation and drying, xerogel samples were heated (about 3 °C/h) in oxygen up to 1050 °C to induce SnO_2 nanoclustering and silica densification.[21] Optical-grade bulk samples about 1 mm thick were finally obtained. Reference samples of Er-doped silica and Er-doped SnO_2 micropowder were also prepared. Erbium concentration in all final samples was measured by x-ray fluorescence. The nanostructure morphology was analyzed by transmission electron microscopy in a previous work.[17] Time-resolved photoluminescence (PL) signals at about 1.5 μm were excited with the third harmonic of a Nd doped yttrium aluminum garnet laser at 355 nm (3.5 eV, pulse rate of 200 Hz) and detected at 300 K by a liquid-nitrogen-cooled photomultiplier tube with high-speed amplifier and a monochromator with bandpass of 1.5 nm. The measurements were performed in photon counting mode using a multichannel scaler and the time resolution was about 10 ns. Electron paramagnetic resonance (EPR) experiments were conducted using a spectrometer in *X* band (9.4 GHz) at 14 K, 18 mW of microwave power, and a modulated field of 0.2 mT, taking care to avoid saturation effects. No signal was detected at 300 K. EPR spectra, taken at fixed modulation and power conditions were normalized with regard to the sample mass.

Figure 1(a) shows the infrared erbium luminescence

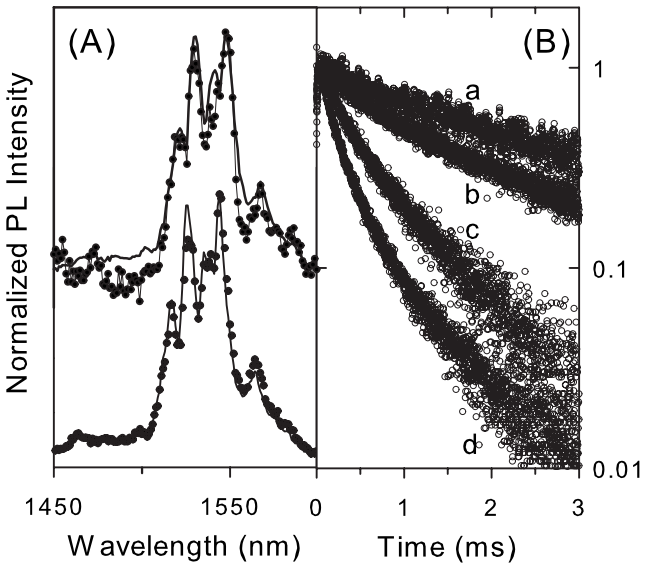

FIG. 1. (a) PL spectra of erbium $^4I_{13/2} \rightarrow {}^4I_{15/2}$ transition excited via FRET from the nanophase (excitation energy, 3.5 eV) with intensity integrated throughout the decay (lower spectra) in samples with 0.01 (circles) and 1.00 mol % Er (full line) and with intensity integrated in selected time windows (upper spectra) from 0.3 to 0.5 ms (circles) and from 1.5 to 3.0 ms (full line) from the excitation pulse in 1.00 mol % Er. (b) Time decay of 3.5 eV excited 1.5 μm PL in samples with 0.05, 0.10, 0.50, and 1.00 mol % from (a) to (d), respectively.

($^4I_{13/2} \rightarrow {}^4I_{15/2}$) in Er-doped SnO_2:SiO_2 excited via energy transfer by nanoparticle excitation in the UV region. The comparison of the observed intensity with that excited in identical conditions in an analogous sample without SnO_2 allows us to estimate an enhancement factor of about 10^2 caused by nanoparticles. The spectra are much more structured, have narrower linewidth than erbium PL in glass,[13] and indicate that the Er^{3+} sites that receive excitation via FRET are located not in an amorphous surrounding but inside the nanocrystals. The excitation at 355 nm indeed allows us to select nanoparticles with not too small size—since the energy gap of small clusters is shifted to higher energy by quantum confinement[14,22]—avoiding the excitation of ions in nanoparticles so small as to be affected by drastic distortions and not negligible interactions with the surrounding glass.[23] In these conditions, spectra collected at increasing delay time after the excitation pulse for samples with largely different erbium content do not show any relevant difference in shape. These observations indicate two important features: the mean environment of the excited ions does not change with the doping level and no other varieties of erbium sites are successively involved during the decay process. The persistence of the spectral band shape, and in particular the absence of the broad band due to the presence of erbium ions in the glass, indicates that excitation transfer from nanophase to glass is negligible and that the excitation diffusion involves only those ions embedded in the nanocrystals. The system behaves, therefore, as an ensemble of disconnected subsets of interacting ions, each able to be excited by the nanoparticle to which it belongs and with a PL kinetics determined by diffusion and decay of the excitation within the single nanoparticle.

However, while the spectra in Fig. 1(a) are independent of time and concentration, the PL decay kinetics of the same samples show a strong dependence on the erbium content, with at least two time regimes [Fig. 1(b)]. The decay is single exponential only at the lowest doping level (0.05 mol %) and with a decay time of about 3 ms, which is equal to the decay time we observed in reference samples of Er-doped SnO_2 powder. The dynamics progressively become multiexponential with increasing Er^{3+} concentration with a concomitant shortening of the asymptotic single-exponential decay time. Even though cooperative up-conversion between nearby erbium ions by dipole-dipole coupling is usually the main concentration-quenching mechanism of erbium luminescence in silica-based glasses—with a marked excitation-density dependence—such process cannot account for the power-independent shortening of the asymptotic decay time reported in Fig. 1(b). This feature points instead to a key role of excitation migration among erbium ions toward acceptor sites where excitation finally undergoes nonradiative decay. Indeed, the decay curves match the expected behavior for diffusion limited relaxation well.[24] In this process, during the initial stage of the decay, excited states are mainly influenced by direct dipolar interactions with nearby acceptors, if any. The initial portion of the decay curves assumes the multiexponential form, $I(t)=I_0 \exp[-(t/\tau_i)-A(t/\tau_i)^{-1/2}]$, where A is a dipolar coupling parameter and τ_i is the intrinsic decay time in the absence of dipolar interactions and diffusion effects.[24] At longer times, excitation migration within the network of neighboring erbium ions becomes the dominating process. This migration indirectly increases the nonradiative deexcitation rate, enhancing the probability of decay in nonradiative defects. As a result, the asymptotic portion of the decay curves is mainly governed by excitation diffusion and the single exponential decay time, τ, is given by contributions from concentration-independent processes and concentration-dependent diffusion-limited mechanisms (with decay times τ_0 and τ_D, respectively) according to the relation $\tau^{-1}=\tau_0^{-1}+\tau_D^{-1}$.[24,25] Therefore, the variation in asymptotic τ in Fig. 1(b) indicates a change in the probability of transferring the excitation to nonradiative acceptors by diffusion. The shortening of the PL lifetime that results from increasing erbium contents points to the important role of erbium ions in the process of excitation diffusion that is confined within the single nanoparticle [Fig. 1(a)]. To draw a more detailed picture of this scenario and determine the dependence of τ on the concentration of the pertinent erbium variety, we need to estimate the fraction of the erbium population belonging to the nanophase and quantify the number of ions per nanoparticle. The identification of the EPR spectrum of erbium in the SnO_2 nanophase has allowed us to accomplish that task.

The EPR spectra we collected at low temperature for SnO_2:SiO_2 [Fig. 2(a)] resemble those reported in other works on Er-doped noncrystalline materials.[26] They consist of a broad, powderlike spectrum a few hundreds mT wide, arising from a strongly anisotropic g tensor with a prominent structure at about 50 mT and a resonance field at about 100 mT. The position of the main resonance ($g \approx 6.7$) indicates that the $^4I_{15/2}$ ground state, which may be expressed in irre-

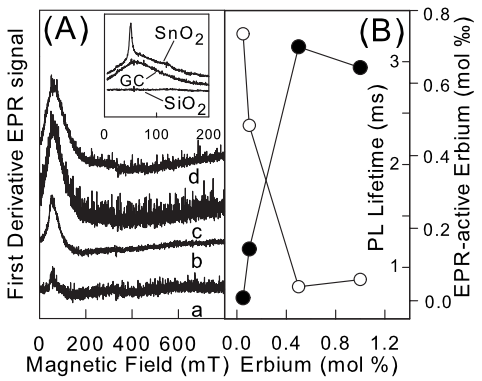

FIG. 2. (a) EPR spectra at 14 K of nanostructured 8 mol % SnO_2:SiO_2 glass ceramics (GC) with different Er dopings of 0.05, 0.1, 0.5, and 1 mol % from (a) to (d), respectively; inset: comparison between EPR spectrum (b) (GC) and spectra of 0.1 mol % Er-doped microcrystalline SnO_2 (SnO_2) and 0.2 mol % Sn-doped glassy silica (SiO_2). (b) EPR-active erbium content (filled circles) and lifetime of the erbium 1.5 μm light emission (open circles) as a function of the total erbium content.

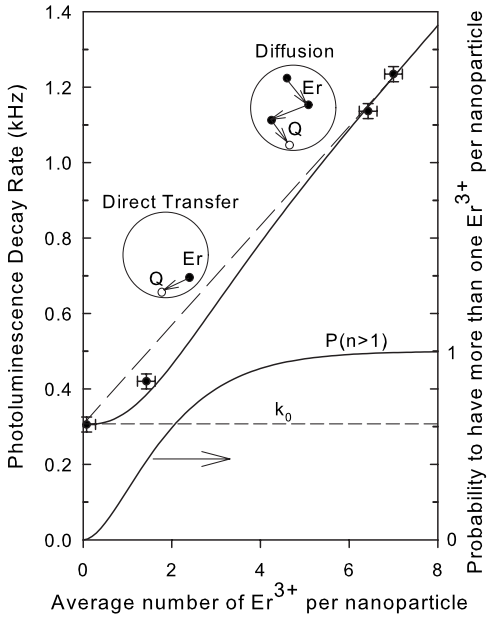

FIG. 3. Decay rate of Er^{3+} 1.5 μm luminescence excited via energy transfer through SnO_2 nanoparticle excitation vs the average number of erbium ions per nanoparticle (symbols). The curve through the experimental points is the best fit from Eq. (1) (with $\lambda N_q^{np}=0.135$ kHz and k_0 as indicated) compared with the linear behavior (dashed line). The curve related to the right axis (see arrow) is the probability to have more than one Er^{3+} ions per nanoparticle. Sketches of direct and diffusion-related transfer within nanoparticles are reported.

ducible representations as $\Gamma_6+\Gamma_7+3\Gamma_8$ (Ref. 27) is the Γ_6 Kramers doublet in a cubiclike environment.[26–28] The broad spectral features are consistent with Er^{3+} ions in environments with reduced crystallinity.

To identify to which of the two phases, SiO_2 or SnO_2, the EPR-active Er^{3+} ions should be ascribed, we analyzed Er-doped reference samples of Sn-doped silica and microcrystalline (μC) SnO_2 [inset in Fig. 2(a)]. The EPR spectrum of Er^{3+} ions in silica glass is so broadened that it is not distinguishable from the background and therefore excludes the SiO_2 erbium variety as a possible source for the EPR signal in Fig. 2(a). However, Er-doped μC SnO_2 shows a composite signal of two distinct spectral contributions: two narrow peaks (linewidth smaller than 50 mT) with structures at 60 and 120 mT arising from erbium in the crystalline lattice internal to the powder grains and a broad band (more than 100 mT wide) that strongly resembles the signal observed for the nanostructured systems due, in the case of μC SnO_2, to erbium at the grain boundaries where defects and deviations from stoichiometry give rise to regions with reduced crystallinity. So, the EPR spectra of the nanostructured SnO_2:SiO_2 realistically appear as fingerprints of the Er^{3+} variety belonging to the SnO_2 nanophase.

Double integration of the EPR spectra compared with quantitative reference samples (both strong pitch and a calibrated Li_2MnO_3 sample[29]) give us an estimation of the molar concentration of Er^{3+} sites embedded in the nanophase [filled marks in Fig. 2(a)]. We note that erbium ions in nanocrystals are only a minor fraction of the total. It is remarkable that, notwithstanding the relatively high concentration of erbium in glass, no energy transfer to these ions is observed. We also note that the concentration of EPR-active sites is not proportional to the nominal Er doping and reveals a limit to the number of Er^{3+} ions per nanoparticle achievable by this synthetic approach. The observation of a linear dependence of the EPR signal broadening on the integrated intensity (indicating that magnetic dipolar interactions arise from erbium ions homogeneously distributed within the nanocrystals), together with the absence of strong concentration quenching effects on the PL response, suggest that the formation of EPR-silent erbium clusters in the nanophase is negligible. It is noteworthy, on the other hand, that the concentration appears strongly correlated with the variation in the PL asymptotic lifetime, τ [open marks in Fig. 2(a)]. This correlation indicates, once again, that the decay mechanism mediated by excitation diffusion depends not on the whole erbium population but on the number of Er^{3+} ions in the nanoparticles. The decay rate, $k=\tau^{-1}$, is thus expected to follow a relation of the form $k=k_0+\lambda N_{Er}^{np} N_q^{np}$, similar to that obtained for a homogeneous system,[3,24] but where N_{Er}^{np} and N_q^{np} are, respectively, the number of Er^{3+} ions and quenching sites per nanoparticle. The nature of the quenching sites is unknown but they are probably localized at the nanoparticle surface where the crystal-to-glass mismatch is compensated by coordination defects and hydroxyl groups which can activate efficient nonradiative decay channels of erbium excitations.

From the concentration of EPR-active sites and the estimated nanoparticle concentration [about 2×10^{18} cm^{-3} taking a mean nanoparticle radius of 2.5 nm (Refs. 17 and 19)], we may esplicitate the experimental relation between k and N_{Er}^{np} (Fig. 3). This number ranges from less than one to up to 7 Er^{3+} ions per nanoparticle. The number N_q^{np} of quenching centers per nanoparticle might in principle change too, changing the erbium doping, since the erbium content was shown to have a role in the final structure.[17] However, if N_q^{np}

did depend on erbium, k would be a nonlinear function of $N_{\mathrm{Er}}^{\mathrm{np}}$ and would exploit a supralinear (Er-induced defectiveness) or a sublinear (Er-induced defect passivation) behavior which would become more and more evident at increasing erbium content. By contrast, we note that the decay rate increases almost linearly—except for the initial sublinearity we comment below—indicating that the variation in decay kinetics is almost entirely due to the growing number of active ions in the nanoparticle with no relevant effect of Er doping on the number of quenching sites. Nevertheless, as noted above, indication of sublinearity appears in the range of low $N_{\mathrm{Er}}^{\mathrm{np}}$, where the number of active sites is comparable to, or lower than the number of available nanoparticles. In this regime, the distribution of active sites among the nanoparticles is expected to be strongly affected by the discreteness and rationing of the available space. In particular and similar to sharp events, the probability of having a given number of erbium ions in a nanocrystal should follow a Poisson distribution law with large deviations from the average number $N_{\mathrm{Er}}^{\mathrm{np}}$. Therefore, the probability of having more than one ion per nanoparticle—so as to have the onset of diffusion effects—needs to be accounted for in order to weight the diffusion limited contribution to the decay rate, k. This probability is given by $P(n>1)=1-\Sigma_{n=0}^{1}P(n)$, where $P(n)=(N_{\mathrm{Er}}^{\mathrm{np}})^{n}\exp(-N_{\mathrm{Er}}^{\mathrm{np}})/(n!)$ is the Poisson function describing the probability of having n events (i.e., n Er^{3+} ions per nanoparticle) when the average number of events is $N_{\mathrm{Er}}^{\mathrm{np}}$ (Fig. 3). As a result, we obtain a relation for k in disconnected nanosized systems:,

$$k = k_0 + \lambda N_{\mathrm{Er}}^{\mathrm{np}} N_q^{\mathrm{np}} [1 - (1 + N_{\mathrm{Er}}^{\mathrm{np}}) e^{-N_{\mathrm{Er}}^{\mathrm{np}}}]. \quad (1)$$

The agreement between Eq. (1) and the experimental data (Fig. 3), with only the $\lambda N_q^{\mathrm{np}}$ factor as an adjustable parameter, suggests that the sublinearity observed at low Er doping in the investigated materials may be evidence of the particular regime imposed on the excitation diffusion by the spatial confinement in disconnected nanosystems. The threshold value of at least two ions per nanoparticle for the onset of diffusion processes, introduced through the $P(n>1)$ function, is also consistent with the ratio—close to 1—between nanoparticle size and Förster radius in the specific material.

In summary, we have demonstrated the feasibility of nanostructured composites in which the excitation of light-emitting sites in nanocrystals is negligibly affected by excitation diffusion outside the nanophase. Effects ascribable to the discrete spatial domain where the excitation diffusion occurs are observed and described by means of a nonlinear relation between photoluminescence decay rate and the average number of active ions per nanoparticle.

We acknowledge the financial support of the Cariplo Foundation, Italy under Project No. 20060656.

[1] J. R. Lakowicz, *Principles of Fluorescence Spectroscopy* (Kluwer Academic, Plenum, New York, 1999), p. 367.
[2] J. R. Silvius and I. R. Nabi, Mol. Membr Biol. **23**, 5 (2006).
[3] D. Pacifici, G. Franzo, F. Priolo, F. Iacona, and L. Dal Negro, Phys. Rev. B **67**, 245301 (2003).
[4] H. S. Han, S. Y. Seo, and J. H. Shin, Appl. Phys. Lett. **79**, 4568 (2001).
[5] N. Daldosso, D. Navarro-Urrios, M. Melchiorri, L. Pavesi, F. Gourbilleau, M. Carrada, R. Rizk, C. Garcia, P. Pellegrino, B. Garrido, and L. Cognolato, Appl. Phys. Lett. **86**, 261103 (2005).
[6] F. Iacona, D. Pacifici, A. Irrera, M. Miritello, G. Franzo, F. Priolo, D. Sanfilippo, G. Di Stefano, and P. G. Fallica, Appl. Phys. Lett. **81**, 3242 (2002).
[7] D. Pacifici, A. Irrera, G. Franzo, M. Miritello, F. Iacona, and F. Priolo, Physica E **16**, 331 (2003).
[8] P. G. Kik, M. L. Brongersma, and A. Polman, Appl. Phys. Lett. **76**, 2325 (2000).
[9] G. Franzo, D. Pacifici, V. Vinciguerra, F. Priolo, and F. Iacona, Appl. Phys. Lett. **76**, 2167 (2000).
[10] C. E. Chryssou, A. J. Kenyon, T. S. Iwayama, C. W. Pitt, and D. E. Hole, Appl. Phys. Lett. **75**, 2011 (1999).
[11] P. G. Kik and A. Polman, J. Appl. Phys. **88**, 1992 (2000).
[12] M. Fujii, M. Yoshida, Y. Kanzawa, S. Hayashi, and K. Yamamoto, Appl. Phys. Lett. **71**, 1198 (1997).
[13] S. Brovelli, N. Chiodini, A. Lauria, F. Meinardi, and A. Paleari, Phys. Rev. B **73**, 073406 (2006).
[14] A. C. Yanes, J. J. Velazquez, J. del-Castillo, J. Mendez-Ramos, and V. D. Rodriguez, Nanotechnology **19**, 295707 (2008).
[15] J. del-Castillo, V. D. Rodriguez, A. C. Yanes, and J. Mendez-Ramos, J. Nanopart. Res. **10**, 499 (2008).
[16] S. Brovelli, N. Chiodini, A. Lauria, F. Meinardi, and A. Paleari, Solid State Commun. **138**, 574 (2006).
[17] S. Brovelli, A. Baraldi, R. Capelletti, N. Chiodini, A. Lauria, M. Mazzera, A. Monguzzi, and A. Paleari, Nanotechnology **17**, 4031 (2006).
[18] S. Brovelli, N. Chiodini, F. Meinardi, A. Lauria, and A. Paleari, Appl. Phys. Lett. **89**, 153126 (2006).
[19] S. Brovelli, N. Chiodini, A. Lauria, and A. Paleari, J. Nanopart. Res. **10**, 737 (2008).
[20] A. Polman, Physica B **300**, 78 (2001).
[21] N. Chiodini, F. Meinardi, F. Morazzoni, J. Padovani, A. Paleari, R. Scotti, and G. Spinolo, J. Mater. Chem. **11**, 926 (2001).
[22] N. Chiodini, A. Paleari, D. Di Martino, and G. Spinolo, Appl. Phys. Lett. **81**, 1702 (2002).
[23] A. C. Yanes, J. del-Castillo, M. Torres, and J. Peraza, Appl. Phys. Lett. **85**, 2343 (2004).
[24] M. J. Weber, Phys. Rev. B **4**, 2932 (1971).
[25] M. Yokota and O. Tanimoto, J. Phys. Soc. Jpn. **22**, 779 (1967).
[26] G. Dantelle, M. Mortier, and D. Vivien, Phys. Chem. Chem. Phys. **9**, 5591 (2007).
[27] A. Abragam and B. Bleaney, *Electron Paramagnetic Resonance of Transition Ions* (Clarendon, Oxford, 1970).
[28] J. D. Carey, R. C. Barklie, J. F. Donegan, F. Priolo, G. Franzo, and S. Coffa, Phys. Rev. B **59**, 2773 (1999).
[29] V. Massarotti, D. Capsoni, M. Bini, C. B. Azzoni, and A. Paleari, J. Solid State Chem. **128**, 80 (1997).